

Chapter - V

Free Convective Heat Transport in a Porous Media bounded by an isothermal vertical plate with thermal Radiation and Magnetohydrodynamic effects: An Exact Solution

Some part of this chapter has been published in the UGC Approved Journal entitled- IOSR Journal of Applied Physics (IOSR-JAP) Volume 7, Issue 3 Ver. II (May. - Jun. 2015), PP 09-17

5.1 Introduction:

Fluid flow through a porous media has been studied theoretically and experimentally by numerous authors due to its wide applications in various fields such as diffusion technology, transpiration cooling, hemodialysis processes, flow control in nuclear reactors etc. In view of geophysical applications of the flow through porous medium, a series of investigations has been made by Raptis *et al.* (1981-1982), where the porous medium is either bounded by horizontal, vertical surfaces or parallel porous plates. Singh *et al.* (1989) and Lai and Kulacki (1990) investigated the free convective flow past vertical wall. Nield (1994) studied convection flow through porous medium with inclined temperature gradient. Singh *et al.* (2005) also presented periodic solution on oscillatory flow through channel in rotating porous medium.

Further due to increasing scientific and technical applications on the effect of radiation on flow characteristic has more importance in many engineering processes occurs at very high temperature and acknowledge radiative heat transfer such as nuclear power plant, gas turbine and various propulsion devices for aircraft, missile and space vehicles. The effect of radiation on flow past different geometry a series of investigation has been made by Hassan (2003), Seddeek (2000) and Sharma *et al.* (2011). The combined radiation–convection flows were extended by Ghosh and Be'g (2008) to unsteady convection in porous media. Hossain and Takhar (1996) studied the mixed convective flat plate boundary-layer problem using the Rosseland (diffusion) flux model. Mohammadein *et al.* (1998) studied the radiative flux effects on free convection in the Darcian porous media using the Rosseland model. The transient magnetohydrodynamic free convective flow of a viscous, incompressible, electrically conducting, gray, absorbing–emitting, but non-scattering, optically thick fluid medium which occupies a semi-infinite porous region adjacent to an infinite hot vertical plate moving with a constant velocity is presented by Ahmed and Kalita (2013). Raptis and Perdikis (2004) also discussed analytically the transient convection in a highly porous medium with unidirectional radiative flux. Ghosh and

Pop (2007) studied indirect radiation effects on convective gas flow. Ahmed and Kalita (2013) investigated the effects of chemical reaction as well as magnetic field on the heat and mass transfer of Newtonian two-dimensional flow over an infinite vertical oscillating plate with variable mass diffusion. Ahmed (2014) presented the effects of conduction-radiation, porosity and chemical reaction on unsteady hydromagnetic free convection flow past an impulsively-started semi-infinite vertical plate embedded in a porous medium in presence of thermal radiation. Thakur and Hazarika (2015) studied about the effects of temperature dependent viscosity and thermal conductivity on magnetohydrodynamic unsteady free convective heat and mass transfer flow of an incompressible micropolar fluid through a porous medium along an infinite vertical plate. The thermal radiation and Darcian drag force MHD unsteady thermal-convection flow past a semi-infinite vertical plate immersed in a semi-infinite saturated porous regime with variable surface temperature in the presence of transversal uniform magnetic field have been discussed by Ahmed *et al.* (2014). Hazarika and Doley (2014) presented a numerical study based on finite difference scheme to investigate the effect of variable viscosity and thermal conductivity with chemical reaction on a transient MHD free convective mass transfer flow of an incompressible viscous electrically conducting, Newtonian fluid past a suddenly started infinite vertical plate in presence of appreciable radiation heat transfer with viscous dissipation and Joulian heat and uniform transverse magnetic field.

The present problem is to investigate the effect of magnetic field and radiation on unsteady free convection heat transfer flow of viscous laminar electrically conducting Newtonian radiating fluid past an impulsively started semi-infinite vertical surface in a Darcian porous medium. The analytical solution is obtained using Laplace Transform technique and discussed graphically for various flow parameters.

5.2 Mathematical Formulation:

Considering the magnetohydrodynamic unsteady free convection and heat transfer flow of a viscous, incompressible, electrically conducting, Newtonian fluid past a semi-infinite isothermal vertical plate embedded in a porous media under the influence of the thermal buoyancy. A uniform magnetic field of uniform strength B_0^2 is assumed to be applied normal to the surface. The flow is assumed to be in the \bar{x} -direction, which is taken along the plate in the upward direction and \bar{y} -axis is normal to it. Initially it is assumed that the plate and the fluid are at the same temperature \bar{T} . At time $t > 0$, the plate temperature is instantly raised to $\bar{T}_w > \bar{T}_\infty$ which is thereafter maintained constant, where \bar{T}_∞ is the temperature outside the boundary layer.

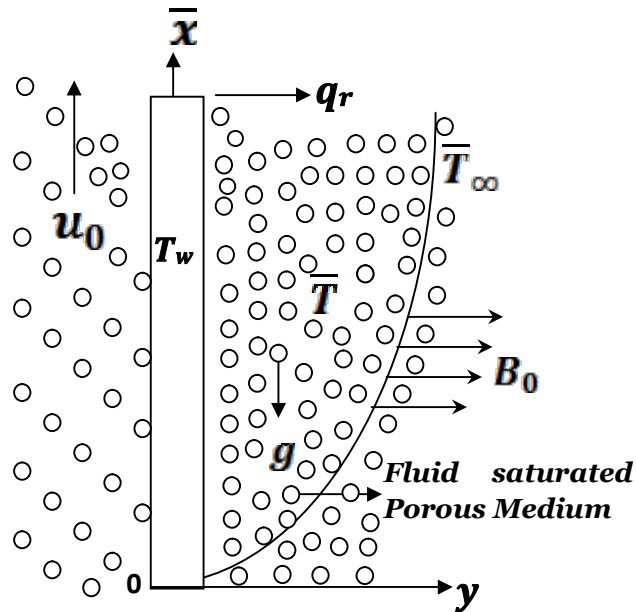


Fig. 5.2 (i): Physical model and coordinate system

The induced magnetic field and viscous dissipation is assumed to be negligible as the magnetic Reynolds number of the flow is taken to be very small. Assuming that the Boussinesq's and boundary-layer approximations hold, the governing equations to the problem are given by:

$$\frac{\partial \bar{u}}{\partial y} = 0 \quad (5.2.1)$$

$$\frac{\partial \bar{u}}{\partial t} = g\beta(\bar{T} - \bar{T}_\infty) + \nu \frac{\partial^2 \bar{u}}{\partial y^2} - \frac{\sigma B_0^2}{\rho} \bar{u} - \frac{\nu}{K} \bar{u}, \quad (5.2.2)$$

$$\rho C_p \frac{\partial \bar{T}}{\partial t} = \kappa \frac{\partial^2 \bar{T}}{\partial y^2} - \frac{\partial q_r}{\partial y}. \quad (5.2.3)$$

The initial and boundary conditions are

$$\left. \begin{aligned} \bar{u} = 0, \bar{T} = \bar{T}_\infty, \forall \bar{y}, \bar{t} \leq 0 \\ \bar{u} = u_0, \bar{T} = \bar{T}_w \text{ at } \bar{y} = 0, \bar{t} > 0 \\ \bar{u} = 0, \bar{T} = \bar{T}_\infty, \text{ as } \bar{y} \rightarrow \infty, \bar{t} > 0 \end{aligned} \right\} \quad (5.2.4)$$

The local radiant absorption for the case of an optically thin gray gas is expressed (Cogley *et.al.* (1968)) as

$$\frac{\partial q_r}{\partial y} = -4\bar{a}\bar{\sigma}(\bar{T}_\infty^4 - \bar{T}^4), \quad (5.2.5)$$

where $\bar{\sigma}$ and \bar{a} are the Stefan-Boltzmann constant and mean absorption co-efficient respectively. We assume that the differences within the flow are sufficiently small so that \bar{T}^4 can be expressed as a linear function of \bar{T} after using Taylor's series to expand \bar{T}^4 about the free stream temperature \bar{T}_∞^4 and neglecting higher order terms. This results in the following approximation:

$$\bar{T}^4 \cong 4\bar{T}_\infty^3\bar{T} - 3\bar{T}_\infty^4, \quad (5.2.6)$$

$$\rho C_p \frac{\partial \bar{T}}{\partial t} = \kappa \frac{\partial^2 \bar{T}}{\partial y^2} - 16\bar{a}\bar{\sigma}\bar{T}_\infty^3(\bar{T} - \bar{T}_\infty). \quad (5.2.7)$$

Introducing the following non-dimensional quantities:

$$\left. \begin{aligned} y &= \frac{\bar{y}u_0\sqrt{G}}{\nu}, \quad u = \frac{\bar{u}}{u_0}, \quad M = \frac{\sigma B_0^2 \nu}{\rho u_0^2 G}, \quad K = \frac{u_0^2 \bar{K}G}{\nu^2}, \quad G = \frac{g\beta\nu(\bar{T}_w - \bar{T}_\infty)}{u_0^3} \\ Pr &= \frac{\mu C_p}{\kappa}, \quad \theta = \frac{\bar{T} - \bar{T}_\infty}{\bar{T}_w - \bar{T}_\infty}, \quad t = \frac{\bar{t}u_0^2 G}{\nu}, \quad R_a = \frac{16\bar{a}\bar{\sigma}\nu^2 \bar{T}_\infty^3}{\kappa u_0^2}, \quad \nu = \frac{\mu}{\rho} \end{aligned} \right\} \quad (5.2.8)$$

Using the transformations (5.2.8), the non-dimensional forms (5.2.2), (5.2.4) and (5.2.7) are

$$\frac{\partial u}{\partial t} = Gr\theta + \frac{\partial^2 u}{\partial y^2} - (M + K^{-1})u, \quad (5.2.9)$$

$$\frac{\partial \theta}{\partial t} = \frac{1}{Pr} \frac{\partial^2 \theta}{\partial y^2} - \frac{R_a}{Pr} \theta. \quad (5.2.10)$$

The corresponding initial and boundary conditions transformed to:

$$\left. \begin{aligned} u &= 0, \theta = 0, \forall y, t \leq 0 \\ u &= 1, \theta = 1 \text{ at } y = 0, t > 0 \\ u &= 0, \theta = 0, \text{ as } y \rightarrow \infty, t > 0 \end{aligned} \right\} \quad (5.2.11)$$

5.3 Method of solution:

The unsteady, non-linear, coupled partial differential equations (5.2.9) and (5.2.10) along with their boundary conditions (5.2.11) have been solved analytically using Laplace transforms technique and their solutions are as follows:

$$u(y,t) = \frac{1}{2} \left[\begin{aligned} & \left(1 - \frac{1}{\psi} \right) \left\{ e^{2\eta\sqrt{\xi}} \operatorname{erfc}(\eta + \sqrt{\xi}t) + e^{-2\eta\sqrt{\xi}} \operatorname{erfc}(\eta - \sqrt{\xi}t) \right\} \\ & + \frac{1}{\psi} e^{\lambda t} \left\{ e^{2\eta\sqrt{(\xi+\lambda)t}} \operatorname{erfc}(\eta + \sqrt{(\xi+\lambda)t}) \right. \\ & \quad \left. + e^{-2\eta\sqrt{(\xi+\lambda)t}} \operatorname{erfc}(\eta - \sqrt{(\xi+\lambda)t}) \right\} \\ & + \frac{1}{\psi} \left\{ e^{2\eta\sqrt{R_a t}} \operatorname{erfc}(\eta\sqrt{\operatorname{Pr}} + \sqrt{R_a t}) + e^{-2\eta\sqrt{R_a t}} \operatorname{erfc}(\eta\sqrt{\operatorname{Pr}} - \sqrt{R_a t}) \right\} \\ & - \frac{1}{\psi} e^{\lambda t} \left\{ e^{2\eta\sqrt{(R_a+\lambda)t}} \operatorname{erfc}(\eta\sqrt{\operatorname{Pr}} + \sqrt{(R_a+\lambda)t}) \right. \\ & \quad \left. + e^{-2\eta\sqrt{(R_a+\lambda)t}} \operatorname{erfc}(\eta\sqrt{\operatorname{Pr}} - \sqrt{(R_a+\lambda)t}) \right\} \end{aligned} \right], \quad (5.3.1)$$

$$\theta(y,t) = \frac{1}{2} \left\{ e^{2\eta\sqrt{R_a t}} \operatorname{erfc}(\eta\sqrt{\operatorname{Pr}} + \sqrt{R_a t}) + e^{-2\eta\sqrt{R_a t}} \operatorname{erfc}(\eta\sqrt{\operatorname{Pr}} - \sqrt{R_a t}) \right\}, \quad (5.3.2)$$

Where $\xi = M + K^{-1}$, $\eta = \frac{y}{2\sqrt{t}}$, $\psi = \xi - R_a$, $\lambda = \frac{\psi}{\operatorname{Pr}-1}$., erf = error function, erfc

= complementary error function.

Skin friction and Nusselt number

The non-dimensional skin friction and Nusselt number is given as follows:

$$\begin{aligned}
\tau &= - \left[\frac{\partial u(y,t)}{\partial y} \right]_{y=0} \\
&= \left(1 - \frac{1}{\psi} \right) \left\{ \frac{e^{-\xi t}}{\sqrt{\pi t}} + \sqrt{\xi} \operatorname{erf} \left(\sqrt{\xi t} \right) \right\} \\
&\quad + \frac{1}{\psi} e^{\lambda t} \left\{ \frac{e^{-(\xi+\lambda)t}}{\sqrt{\pi t}} + \sqrt{(\xi+\lambda)} \operatorname{erf} \left(\sqrt{(\xi+\lambda)t} \right) \right\} \\
&\quad + \frac{1}{\psi} \sqrt{Pr} \left\{ \frac{e^{-R_a t}}{\sqrt{\pi t}} + \sqrt{R_a} \operatorname{erf} \left(\sqrt{R_a t} \right) \right\} \\
&\quad - \frac{1}{\psi} \sqrt{Pr} e^{\lambda t} \left\{ \frac{e^{-(R_a+\lambda)t}}{\sqrt{\pi t}} + \sqrt{(R_a+\lambda)} \operatorname{erf} \left(\sqrt{(R_a+\lambda)t} \right) \right\}
\end{aligned} \tag{5.3.3}$$

$$Nu = - \left[\frac{\partial \theta(y,t)}{\partial y} \right]_{y=0} = \sqrt{Pr} \left\{ \frac{e^{-R_a t}}{\sqrt{\pi t}} + \sqrt{R_a} \operatorname{erf} \left(\sqrt{R_a t} \right) \right\}. \tag{5.3.4}$$

5.4 Results and Discussion:

The problem of thermal radiation effect on a porous media transport under optically thin approximation has been formulated, analyzed and solved analytically. In order to point out the effects of physical parameters namely; magnetohydrodynamic force (M), radiation parameter (R_a), Porosity parameter (K) on the flow patterns, the computation of the flow fields are carried out. The values of velocity, temperature, shear stress and rate of heat transfer are obtained for the physical parameters as mention. The velocity profiles have been studied and presented in Figs. 5.4 (i) to 5.4 (iii). Figure 5.4 (i) shows the effect of the Hartmann number M on the fluid velocity and the results show that the presence of the magnetic force causes retardation of the fluid motion represented by general decreases in the fluid velocity. It is due to the fact that the magnetic force which is applied in the normal direction to the flow produces a drag force which is known as Lorentz force. The opposite trend is observed in Figure 5.4 (ii) for the case when the

values of the porous permeability ($K = 0.2, 0.5, 1.0, 1.5$) are increased. As depicted in this figure, the effect of increasing the value of porous permeability is to increase the value of the velocity component in the boundary layer due to the fact that drag is reduced by increasing the value of the porous permeability on the fluid flow which results in increased velocity. This trend shows that the velocity is accelerated with increasing porosity parameter. The effect of radiation ($R_a = 0, 15, 16, 18$) for the velocity profiles is presented in Figure 5.4 (iii). It is observed that the flow velocity is accelerated with increasing values of radiation. Also it is seen that without radiation ($R_a = 0$, Figure 5.4 (iii)) or for the small value $K = 0.2$ (Figure 5.4 (ii)), the values of flow velocity is reduced exponentially from the plate, whereas for the higher values of K or R_a the flow velocity has a bigger pick in the neighbourhood of $y = 0.2$, but the opposite behaviour has been observed for the effects of higher magnetohydrodynamic force ($M = 10$, Figure 5.4 (i)).

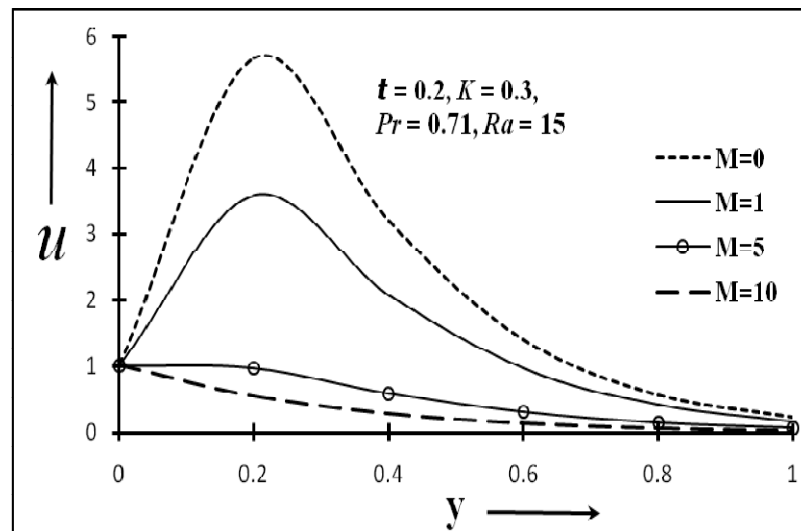


Fig. 5.4 (i): Flow velocity distribution for Hartmann number M

The temperature profiles are calculated for different values of thermal radiation parameter ($R_a = 0, 5, 10, 15$) at time $t = 0.2$ and these are shown in Figure

5.4(iv). The effect of thermal radiation parameter is important in temperature profiles. It is observed that the decreasing radiation parameter increases temperature. Figure 5.4(v) reveals temperature variations with Pr (Prandtl number) which signifies the ratio of momentum to thermal diffusivity at $t = 0.2$. The temperature is observed to decrease with an increase in Pr . For lower Pr fluids, heat diffuses faster than momentum and vice versa for higher Pr fluids. Larger Pr values correspond to a thinner thermal boundary layer thickness and more uniform temperature distributions across the boundary layer. Smaller Pr fluids possess higher thermal conductivities so that heat can diffuse away from the vertical surface faster than for higher Pr fluids (low Pr fluids correspond to thicker boundary layers). For working oils ($Pr = 11.4$), convection is very effective in transferring energy from an area, compared to pure conduction and momentum diffusivity is dominant. It is also observed that the temperature is maximum near the plate and decreases away from the plate and finally takes asymptotic values for all values of Pr .

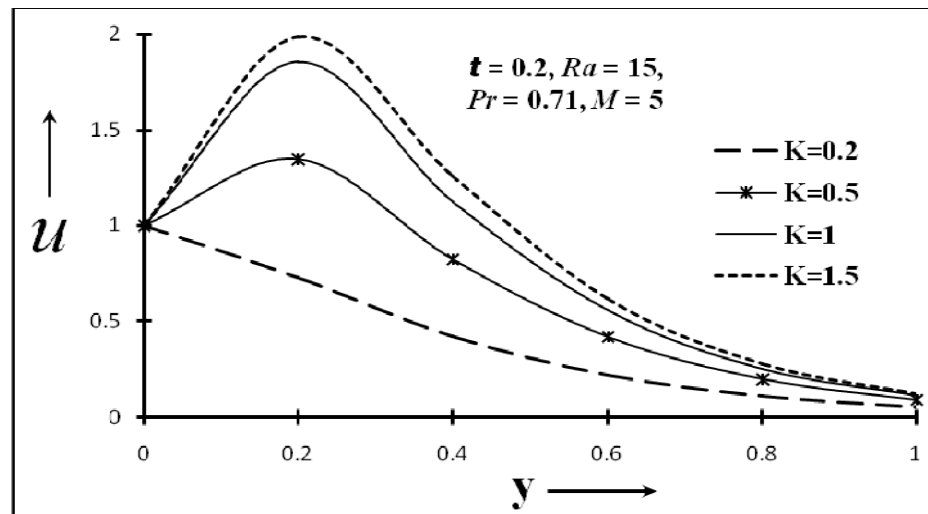


Fig. 5.4 (ii): Flow velocity distribution for porosity K

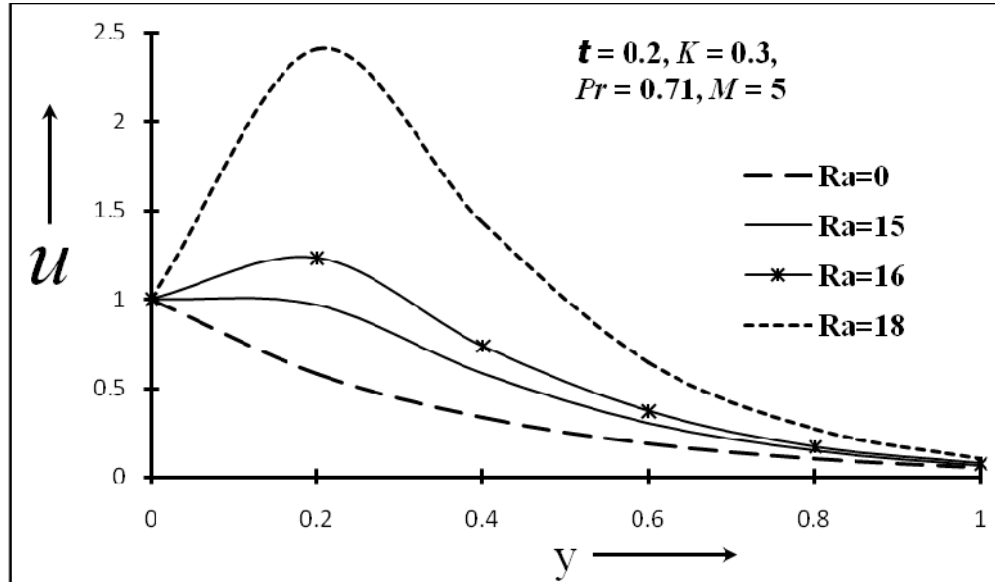


Fig.5.4 (iii): Flow velocity distribution for radiation Ra

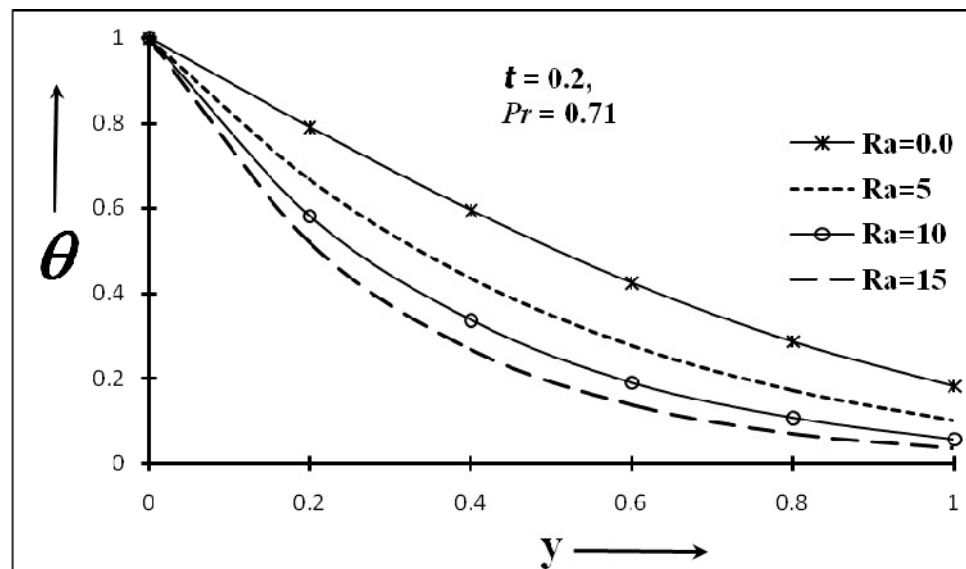


Fig. 5.4 (iv): Temperature distribution for radiation Ra

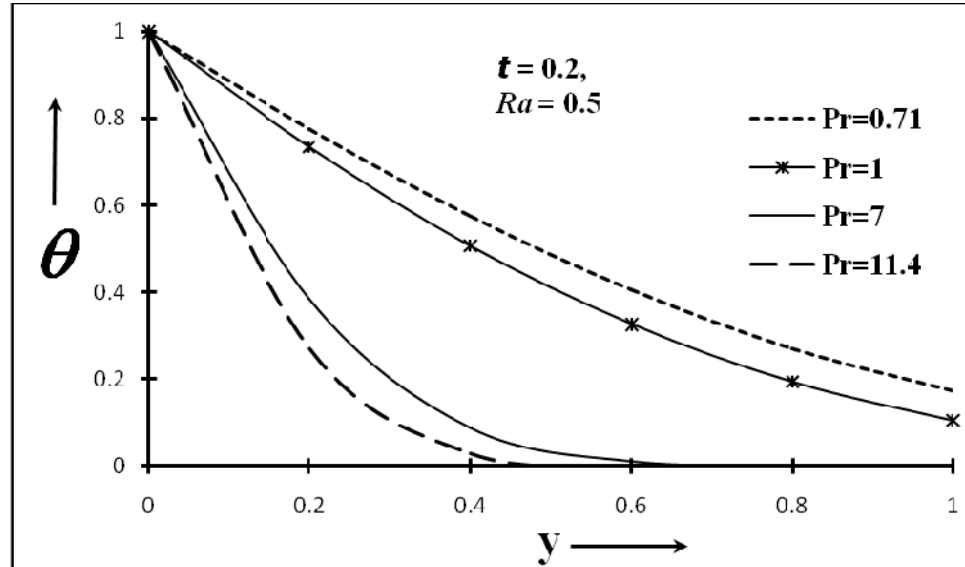


Fig. 5.4 (v): Temperature distribution for Pr

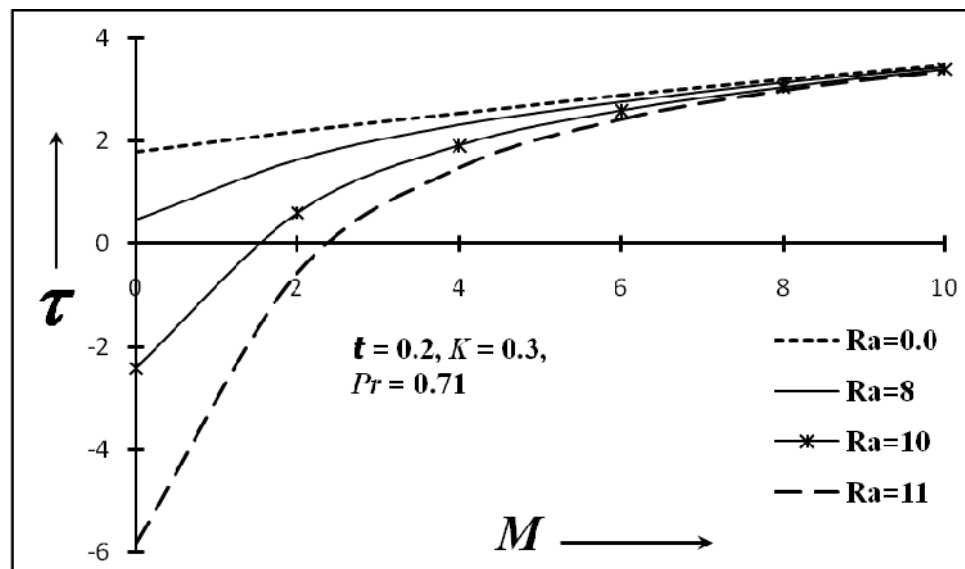


Fig. 5.4 (vi): Skin friction distribution for radiation Ra

Figure 5.4 (vi) illustrates the transient shear stress variation with Hartmann number and radiation parameter. The shear stresses at the wall are seemed to be enhanced with a rise in Hartmann number, which is proportional to the square of the magnetic field, B_0 . A reversed trend has been observed for conduction-radiation on shear stress (τ) that means τ is decreased substantially at the wall for $R_a = 0, 8, 10, 11$. For the non-radiating flow case $R_a = 0$, a significant linear flow of shear stress is sustained against hydromagnetic force. For the case, $R_a = 10, 11$ a significant flow reversal (backflow) is obtained within the region $0 < M < 2.5$ i.e. shear stresses become negative. However for $R_a = 0, 8$ all backflow is eliminated entirely from the regime for all hydromagnetic forces and only positive shear stresses arise at the plate.

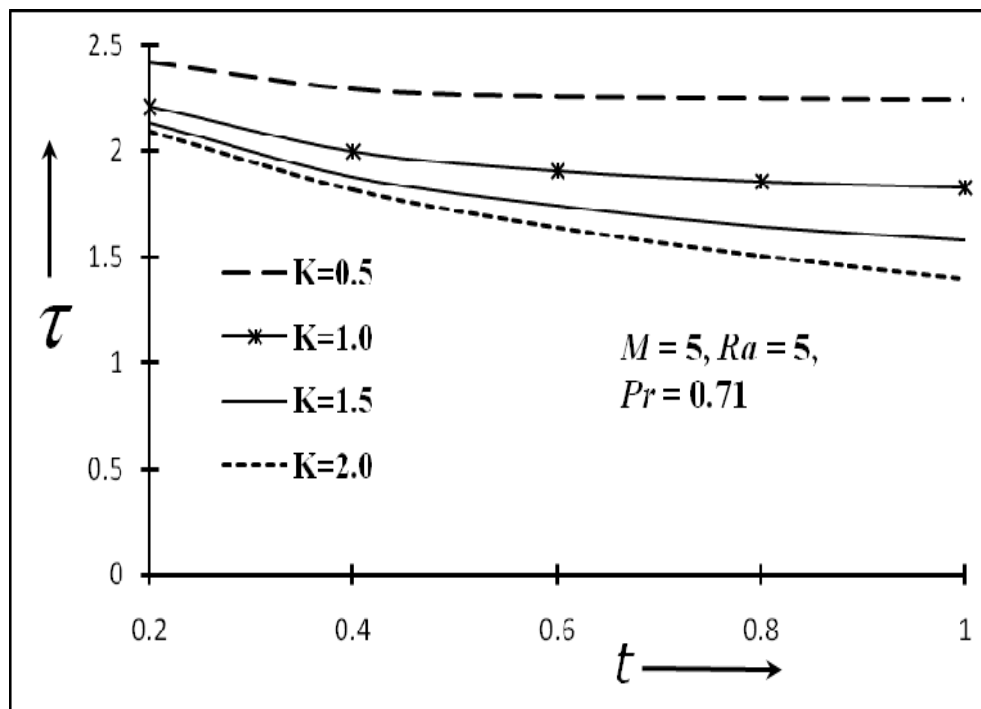


Fig. 5.4 (vii): Skin friction distribution for K

Figure 5.4 (vii) shows the distribution of shear stress at the wall for various porosity parameters over time. With a rise in porosity parameter K , from 0.5, 1.0 through 1.5 to 2.0 decreases the magnitude of the shear stress through the boundary layer. We observe that for all values of K , shear stress remains positive i.e. no flux reversal arises for all times into the boundary layer. With progression in time t , the shear stress is however found to decrease continuously.

Finally, in Fig. 5.4(viii) the distribution of rate of heat transfer with radiation parameter is shown against t . Inspection shows that, increasing radiation parameter R_a , tends to boost the heat transfer rate at the wall i.e. elevate Nu magnitudes. A substantial decrease is observed in Nu for the time parameter.

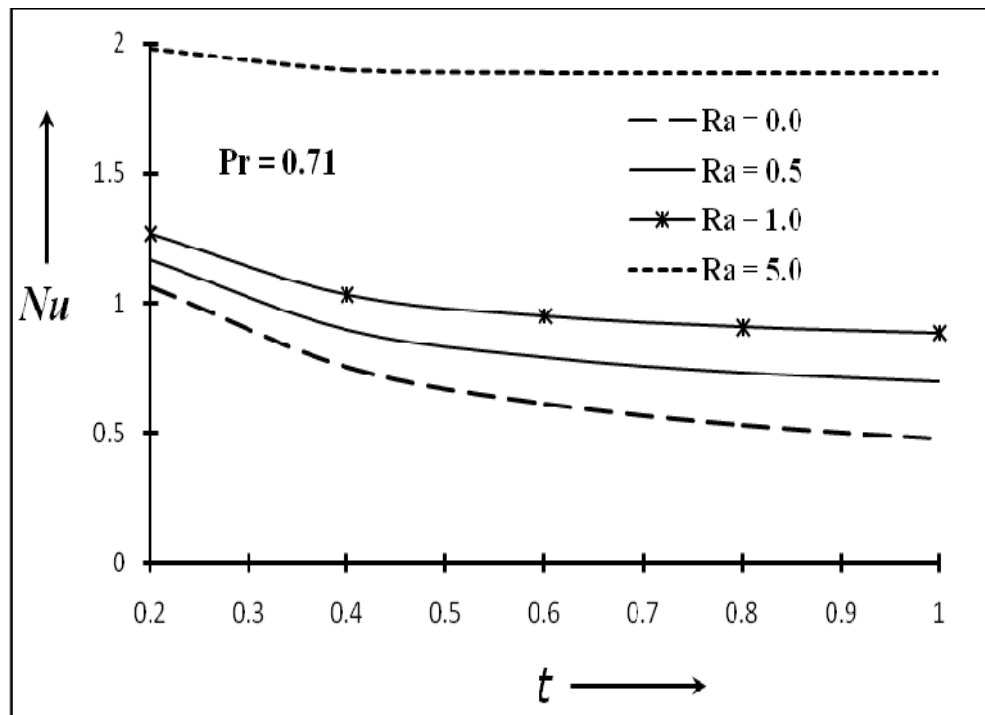


Fig. 5.4 (viii): Nusselt number distribution for radiation R_a

5.5 Conclusions:

In the present work, we have analyzed flow, heat transfer on convection flow of a viscous, incompressible, electrically conducting and radiating fluid over an infinite vertical plate embedded in a Darcian porous regime in the presence of transverse magnetic field and thermal radiation using the classical model for the radiative heat flux. Final results are computed for variety of physical parameters which are presented by means of graphs. Laplace transforms solutions for the non-dimensional momentum and energy equations subject to transformed boundary conditions have been obtained and the results indicate that:

- The flow has been shown to be decelerated with increasing Hartmann number but accelerated with conduction-radiation and porosity parameters.
- Increasing Hartmann number also increases the shear stress and back flow has been observed for higher radiation near the wall.
- A positive decrease in R_a or K strongly enhanced the shear stress.
- Increasing thermal radiation contribution (R_a) serves to enhance wall heat transfer gradient significantly in the porous regime.
- With an increase in time (t), both the skin friction and wall heat transfer are decreased.
- Temperature is decreased with an increase in thermal radiation contribution (R_a).

The study has important applications in materials processing and nuclear heat transfer control, as well as MHD energy generators. The current study has employed a Newtonian viscous model. Presently the authors are extending this work to consider viscoelastic fluids and also power-law rheological fluids. The results of these studies will be presented imminently.